Beyond threshold hillslopes: Channel adjustment to base-level fall in tectonically active mountain ranges

William B. Ouimet[1], Kelin X Whipple[2], and Darryl E. Granger[3]
[1]Department of Geology, Colorado College, Colorado Springs, Colorado 80903, USA
[2]School of Earth and Space Exploration, Arizona State University, Tempe, Arizona 85287-1404, USA
[3]Department of Earth and Atmospheric Sciences, Purdue University, West Lafayette, Indiana 47907, USA

ABSTRACT

Numerous empirical and model-based studies argue that, in general, hillslopes and river channels increase their gradients to accommodate high rates of base-level fall. To date, however, few data sets show the dynamic range of both these relationships needed to test theoretical models of hillslope evolution and river incision. Here, we utilize concentrations of ^{10}Be in quartz extracted from river sand on the eastern margin of the Tibetan Plateau to explore relationships among short-term (10^2–10^5 a) erosion rate, hillslope gradient, and channel steepness. Our data illustrate nonlinear behavior and a threshold in the relationship between erosion rate and mean hillslope gradient, confirming the generalization that hillslopes around the world are limited by slope stability and cease to provide a metric for erosion at high rates (>~0.2 mm/a). The relationship between channel steepness index and erosion rate is also nonlinear, but channels continue to steepen beyond the point where threshold hillslopes emerge up to at least 0.6 mm/a, demonstrating that channel steepness is a more reliable topographic metric than mean hillslope gradient for erosion rate and that channels ultimately drive landscape adjustment to increasing rates of base-level fall in tectonically active settings.

INTRODUCTION

Quantitative knowledge of the relation between topographic morphology and erosion rate is central to testing landform evolution theories and addressing questions about potential coupling between erosion and tectonics. Topographic metrics of erosion rate that have been discussed in the literature include mean hillslope gradient, local relief, and channel steepness normalized for drainage area. Many studies have focused on the relationship between mean hillslope gradient and erosion rate (e.g., Granger et al., 1996; Binnie et al., 2007), but surprisingly little analysis about the ways in which these data compare to theoretical models has been published. Moreover, as erosion rates increase, it has long been argued that average hillslope gradient within a landscape should approach a threshold value controlled by slope stability and cease to provide a metric for erosion rates (e.g., Strahler, 1950; Burbank et al., 1996; Montgomery and Brandon, 2002). This threshold is thought to be reached wherever erosion rate exceeds the surface soil production rate (typically <~0.2 mm/a; Heimsath et al., 1997), limiting the value of relations between hillslope gradient and erosion rate for tectonic interpretation and studies of the coupling between climate and tectonics. Nevertheless, for understanding soil-mantled landscapes, there is a need to expand the available database on hillslope morphology as a function of erosion rate and to use these data to test existing hillslope evolution models.

Much less has been published on the relation between the channel steepness index and erosion rate, despite frequent arguments that channel steepness largely sets kilometers-scale relief and provides a more reliable metric of erosion rates than mean hillslope gradient in tectonically active landscapes (e.g., Wobus et al., 2006). Although many studies have shown correlations between erosion rate and various measures of topographic relief (e.g., Montgomery and Brandon, 2002; von Blanckenburg, 2005, and references therein), relatively limited data exist to evaluate the hypothesis that variations in channel steepness ultimately drive these correlations and to test river incision models (e.g., Lavé and Avouac, 2001; Snyder et al., 2003; Wobus et al., 2006; Whittaker et al., 2007). Moreover, for a great many problems in tectonic geomorphology, such as those concerning the potential coupling between climate and tectonics, controls on orogen response time to climatic or tectonic perturbation, controls on the heights of mountain ranges, and the longevity of mountainous topography, we need field data on the relationship between the channel steepness index and erosion rate, particularly in the landslide-dominated settings that characterize many tectonically active mountain ranges (e.g., Burbank et al., 1996). Key questions include: (1) does channel steepness encode information about erosion rates beyond the point where threshold hillslopes emerge, (2) what is the form of the relation between erosion rate and channel steepness, and (3) is there a threshold to channel steepness?

In this paper, we present data from 65 basins on the eastern margin of the Tibetan Plateau that span a wide range of erosion rates and topographic morphologies, augmenting available data on hillslope gradient and providing critical new data on channel steepness index as a function of erosion rate.

EASTERN MARGIN OF THE TIBETAN PLATEAU

The eastern margin of the Tibetan Plateau is a transient landscape, characterized by a regionally persistent, elevated, low-relief relict landscape that has been deeply dissected by major rivers and their tributaries (Clark et al., 2006). Rates of rock cooling in the region increased dramatically between 9 and 13 Ma, suggesting that regional uplift and trunk river incision began at that time (Clark et al., 2005; Ouimet, 2007). Major rivers start at high elevations over 4000 m, where they are slightly incised into this relict landscape and become subsequently more deeply incised as they flow downstream. Lower reaches of these main-stem rivers are characterized as rapidly incising, high-relief gorges with steep hillslopes where large landslides are common (Ouimet et al., 2007).

Our work is focused within the drainage basins of Dadu, Yalong, and Min Rivers in Sichuan province, China (Fig. 1). Bedrock geology consists mainly of the Songpan-Ganze flysch, which is intruded by a series of Jurassic age granitic plutons, and it also includes deformed Paleozoic rocks and crystalline Precambrian basement that outcrop in the southern portions of each drainage basin. The field area experiences a moderate subtropical monsoon in the summer months. Annual precipitation varies from ~300–600 mm/a over most of the field area, but it ranges up to ~1000–1500 mm/a in isolated areas adjacent to the Sichuan Basin.

COSMOGENIC AND TOPOGRAPHIC ANALYSIS

We quantified basin-averaged erosion rates using in situ cosmogenic ^{10}Be in quartz extracted from river sand. ^{10}Be accumulates at Earth's surface proportional to its local production rate and inversely proportional to erosion rate. If sand collected at a stream outlet provides a representative mixture of sand generated from erosion throughout a basin (least likely at the highest erosion rates; Bierman and Steig, 1996), this method yields erosion rates averaged over the time to erode one *e*-folding penetration length of ^{10}Be production by neutron spallation (~60 cm in rock). This technique has been shown to yield reliable short-term (10^2–10^5 a) basin-averaged erosion rates in many different tectonic and climatic settings

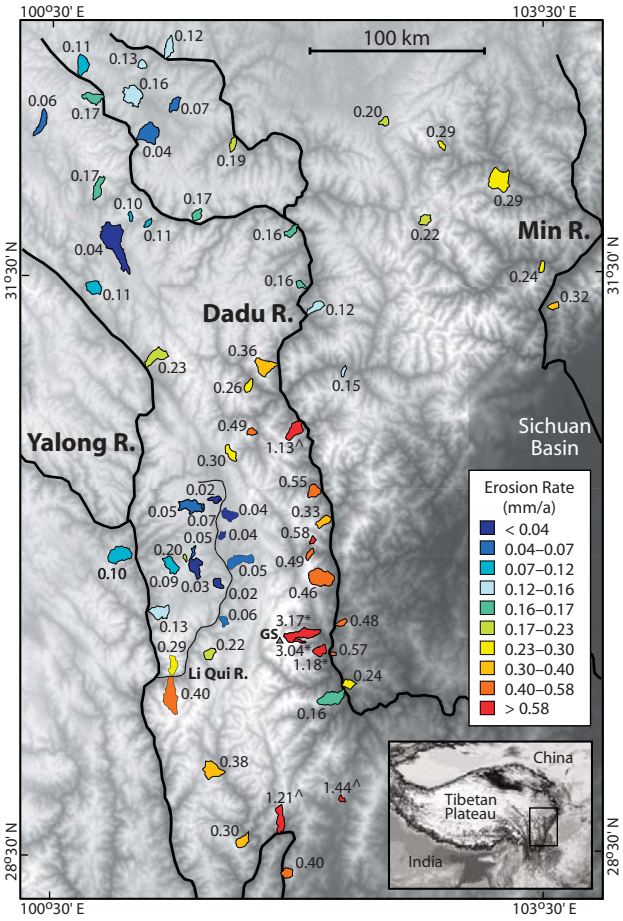

Figure 1. Study area, sample basins, and measured erosion rates. Symbol ^ denotes erosion rate outliers; * denotes glaciated basins near Gongga Shan (GS), as discussed in text. Underlying topography is GTOPO30 (U.S. Geological Survey).

(e.g., Bierman and Nichols, 2004; von Blanckenburg, 2005, and references therein).

We collected river sand from 65 tributary basins within the Dadu, Yalong, and Min River drainages (Fig. 1; Table DR1 in the GSA Data Repository[1]). Our sampling strategy was to carefully select basins following several criteria to ensure confident interpretation of measured ^{10}Be concentrations as well-mixed, mean basinwide erosion rates. These criteria included sampling basins that: (1) drain a relatively uniform, quartz-rich bedrock lithology (mainly granite or metamorphosed sandstone flysch); (2) display minimal Pleistocene glacial modification; (3) have only small volumes of sediment stored in terraces; (4) do not exhibit evidence of recent large-magnitude floods or debris flows that might deliver poorly mixed sands to the basin outlet; (5) do not show signs of recent large, deep-seated bedrock landslides; (6) are large enough (>25 km^2) to allow appropriate mixing of sediments from shallow landslides (Niemi et al., 2005) and anthropogenic disturbances (farming, roads, mining, etc.); and (7) are small enough (<100–200 km^2) to ensure as much as possible uniform topographic and geologic characteristics.

[1]GSA Data Repository item 2009137, data tables, full methodology for cosmogenic and topographic analysis, and additional details for the hillslope evolution models discussed in the text, is available online at www.geosociety.org/pubs/ft2009.htm, or on request from editing@geosociety.org or Documents Secretary, GSA, P.O. Box 9140, Boulder, CO 80301, USA.

Sampled basins were also specifically selected to cover a range of topographic characteristics. Main-stem rivers and large tributaries in the field area are in transient states responding to regional uplift (Ouimet et al., 2007). Each basin we sampled, however, is a small side-tributary of the larger rivers that exhibits relatively uniform hillslope gradients and smooth, concave river profiles without knickpoints or significant changes in profile concavity that might suggest strongly nonuniform rates of erosion and ongoing transient adjustment. Thus, while the large rivers as a whole are in transient states, the basins we sampled appear to be adjusted to local, recent main-stem incision rates. We focus on two key measures of topography: mean basin slope and mean basin k_{sn} (a measure of channel steepness, normalized by drainage area) (see the Data Repository material for full methodology). Sampled basins range in mean elevation (1900–4500 m), basin relief (500–3500 m), mean basin slope (~3°–35°), and mean basin k_{sn} (20–500 m$^{0.9}$). Topographic data for all basins are summarized in Table DR1.

SHORT-TERM (10^2–10^5 A) EROSION RATES

Erosion rates range from ~0.03 mm/a to ~3 mm/a, corresponding to average time scales from 27,000 to 200 a, respectively (Fig. 1; Table DR1). The average erosion rate from all basins is 0.36 mm/a, and most (59 of 65) are less than 0.6 mm/a. Erosion rates generally decrease upstream along the Dadu and Yalong Rivers and their large tributaries, but they are uniform within the Min River drainage. The lowest erosion rates (< 0.10 mm/a) occur at high elevations, associated with remnants of an elevated, low-relief relict landscape (Clark et al., 2006). Erosion rates associated with the lower reaches of the Dadu and Yalong Rivers (~0.3–0.5 mm/a) are consistent with long-term incision rates determined from low-temperature thermochronology (0.3–0.4 mm/a) (Clark et al., 2005; Ouimet, 2007).

Between 0.025 and 0.58 mm/a, our data are spread out evenly and cover a wide range of hillslope gradients (~3°–35°) and mean basin k_{sn} values (20–440 m$^{0.9}$). The six erosion rates that are >1 mm/a are from catchments with high mean basin slope (>30°) and mean basin k_{sn} (>300 m$^{0.9}$) values. These six erosion rate estimates have the largest uncertainty associated with them due to the higher uncertainty associated with low ^{10}Be concentrations and the greater likelihood for occurrence of landslides and debris flows leading to poorly mixed stream sediment (e.g., Bierman and Steig, 1996; Niemi et al., 2005). Three of these high rates occur in the vicinity of Gongga Shan (7556 m; GS on Fig. 1), within an ~600 km^2 area that deviates from regional characteristics in terms of having active alpine glaciers as well as higher peak elevations, precipitation, and rates of exhumation. The Gongga Shan basins are thus not comparable to all other sites. The other three erosion rates >1 mm/a are 2–3 times higher than rates in nearby basins, suggesting that they may be outliers.

HILLSLOPE GRADIENT

Our data show a strongly nonlinear relation between average hillslope gradient and short-term erosion rate (Fig. 2A). Erosion rates increase in a roughly linear fashion with mean basin slope from ~5° to 20°, and then they increase rapidly as mean basin slope approaches a threshold near the angle of repose (~32°–35°). Hillslope gradient becomes insensitive to erosion rates in excess of ~0.2–0.25 mm/a (Fig. 2A). This observation, and even these approximate threshold values, are not unexpected (e.g., Burbank et al., 1996), and, indeed, they have been reported in several other landscapes (Granger et al., 1996; Montgomery and Brandon, 2002; von Blanckenburg, 2005; Binnie et al., 2007). Among published data sets, the transition to threshold slopes as erosion rates increase to rates that exceed commonly reported surface soil production rates (with published maxima around 0.2 mm/a; Heimsath et al., 1997) is most convincingly documented in our data and that of Binnie et al. (2007). Consistent with our own field observations and interpretation of satellite imagery, this finding is further supported by observational evidence indicating that this

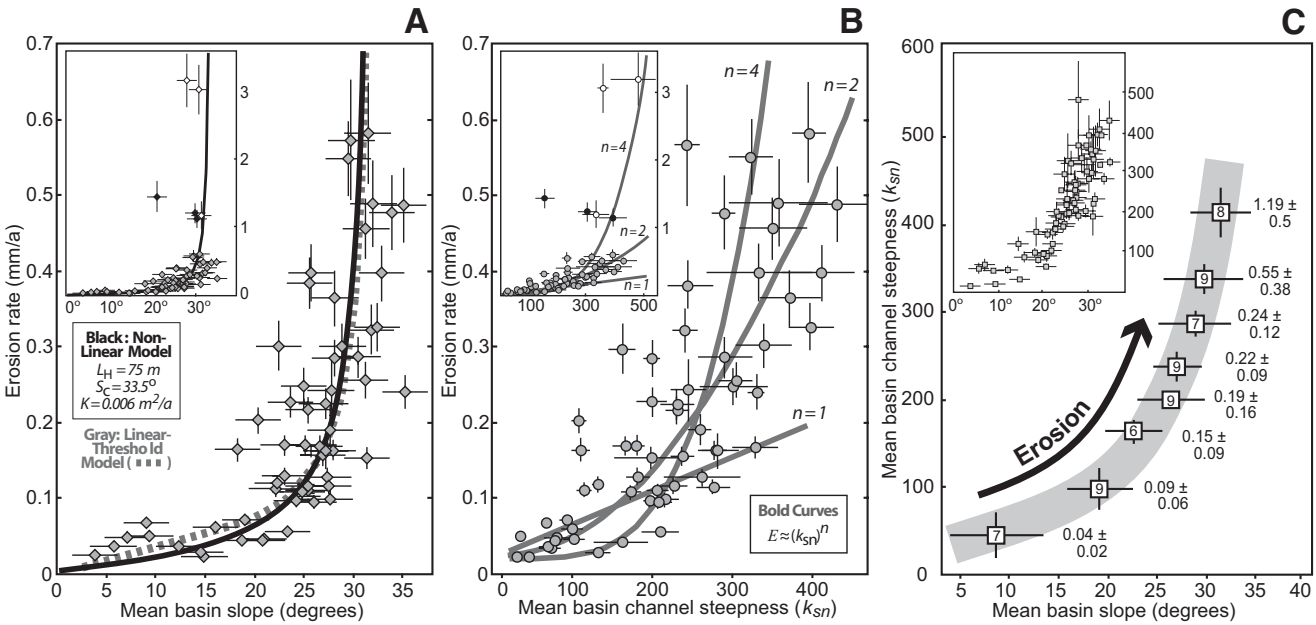

Figure 2. Erosion and topography: main plots in A and B focus on erosion rates <0.6 mm/a (59 basins; gray); insets show full data set (65 basins), including outliers (black) and glaciated basins near Gongga Shan (white). (A) Mean basin slope versus erosion rate. Solid black line is from nonlinear model in Roering et al. (2001) using K, L_H, and S_C values indicated; dashed gray line is from linear-threshold model with L_H = 75 m, K = 0.015 m²/a, and S_C = 32° (see the GSA Data Repository [see footnote 1] for additional details). (B) Mean basin k_{sn} (normalized channel steepness) versus erosion rate. Bold lines depict $E \approx (k_{sn})^n$; n = 1 is a linear relationship between mean basin k_{sn} and erosion rate (E); n = 2 and n = 4 are nonlinear, power-law relationships. (C) Summary plot of binned mean basin slope versus mean basin k_{sn} with average erosion rates indicated (number of data points indicated within box). Inset shows all data points.

threshold is associated with a transition from soil-mantled to rocky landscapes as documented by Binnie et al. (2007).

The most theoretically satisfying, and most fully developed, hillslope transport model consistent with a limiting threshold slope (S_C) and a nonlinear relationship between mean basin slope and erosion rate is the nonlinear hillslope diffusion model of Roering et al. (2001). We cannot, however, a priori reject a simpler model in which soil transport is linearly dependent on slope until a slope-stability threshold is reached, at which point the potential transport rate becomes infinite. Assuming that quasi-equilibrium hillslope morphologies, a hillslope diffusion constant (K), and a hillslope length (L_H) can be used to characterize a basin (Roering et al., 2007), either model can be readily cast as a predicted relationship between mean slope and erosion rate (Fig. 2A). For L_H = 75 m (estimated from satellite imagery and digital elevation models [DEMs]), our data are consistent with model curves based on a reasonable range of K values expected from studies of soil-mantled hillslopes in semiarid to temperate climates (0.002–0.02 m²/a) and S_C (32°–35°). This represents an important confirmation of theoretical models of hillslope evolution and a corroboration of the interpretation of earlier field data.

CHANNEL STEEPNESS INDEX

Assuming that basin-averaged erosion rates reflect the average rate of river incision that drives hillslope base-level fall, the normalized channel steepness index (mean basin k_{sn}) of the well-graded tributary basins sampled in our study can be compared to measured erosion rates. Our data suggest a nonlinear relationship between mean normalized channel steepness and erosion rate (Fig. 2B). This nonlinearity, however, is not as strong as the nonlinearity between mean hillslope gradient and erosion rate. Channels continue to steepen up to ~0.6 mm/a and higher, exceeding the hillslope threshold of ~0.25 mm/a (Figs. 2A and 2B). This is further demonstrated in Figure 2C, which shows the erosion rates associated with different combinations of hillslope gradient and channel steepness index. By the time erosion rates get to 0.20–0.25 mm/a, hillslope gradients have stopped increasing and have reached threshold values (>30°), but channels continue to steepen as erosion increases up to at least 0.6 mm/a (Fig. 2C). This pattern supports the view that beyond the point where threshold hillslopes emerge, river channels continue to steepen in order to incise more rapidly and transport downstream a larger volume of material derived from upstream and adjacent hillslopes.

A linear relationship between k_{sn} and erosion rate has been suggested by data from a few field sites (Safran et al., 2005; Wobus et al., 2006), and this may describe our data at lower values of k_{sn} and erosion rate, but at higher values, the rate of channel steepness increase slows, suggesting that incision becomes more efficient at high channel gradients, similar to the argument made by Snyder et al. (2003) on theoretical grounds and supported by limited field data. Keeping in mind that our highest erosion rates have the greatest uncertainties, include anomalous values in an otherwise systematic pattern consistent with the long-term evolution of landscapes in the field area (Fig. 1), and include basins near the glaciated Gongga Shan area, we focus our interpretation on erosion rates <0.6 mm/a and argue that the relationship between k_{sn} and erosion rate is only mildly nonlinear ($E \approx (k_{sn})^n$ with n = 2; Fig. 2B). We are hesitant to say that our data indicate that this nonlinearity could be much stronger and that the channel steepness index may indeed reach threshold values.

Nonlinear behavior between erosion and channel steepness can arise for a number of reasons. Using the stream-power framework (Whipple and Tucker, 1999), nonlinear behavior ($E \approx (k_{sn})^n$ with n >1) reflects a different erosion process than linear behavior (n = 1). The classic, simplest form of the stream-power model is the linear model (n = 1); the fact that our data are better described by n >1 suggests that the simple linear stream-power model of river incision breaks down at high rates of erosion. One example of nonlinear behavior has been argued to result from the combined effects of a critical threshold of motion and detachment and the probability distribution of flood magnitudes and durations (Snyder et

al., 2003; Lague et al., 2005). These studies suggest that incision becomes more efficient at steeper channel gradients because floods exceed the shear stress thresholds necessary for gravel entrainment and incision more frequently and for longer durations as channel gradient increases.

The variability exhibited in the relationship between mean basin k_{sn} and erosion rate, especially at faster erosion rates and higher values of channel steepness (Fig. 2B), limits our ability to make definitive comparisons between data and various river incision models. The range in channel gradient at any given erosion rate may speak to our initial assumption of quasi-steady incision, the variability of erosion associated with faster erosion and the stochastic nature of landslides (Niemi et al., 2005), or the myriad adjustments in channel morphology (e.g., channel width), bed state (e.g., percent rock exposure, bed material size), hydraulic roughness, and/or dominant incision processes that may accompany changes in channel slope. Unfortunately only sparse data exist to characterize changes in channel morphology and bed state as a function of erosion rate, and both access limitations and the geographic extent of our study area prevented such data collection as part of this study.

CONCLUSIONS

Our data set of cosmogenic erosion rates from the eastern margin of the Tibetan Plateau offers important insight into the ways in which hillslope and river channel morphology change to accommodate higher rates of erosion. The relationship between erosion rate and mean hillslope gradient is strongly nonlinear, indicating that hillslopes in our field area are limited by slope stability and cease to be a topographic metric for erosion rate above 0.2–0.25 mm/a. The relationship between erosion rate and channel steepness index, meanwhile, does not exhibit a clear threshold and is mildly nonlinear. More importantly, this relationship indicates that channels continue to steepen beyond the hillslope threshold up to ~0.6 mm/a, demonstrating that channel steepness is a more reliable topographic metric of erosion than hillslope gradient at high rates in the landslide-dominated, threshold hillslope settings that characterize many tectonically active mountain ranges, and supporting that idea that channels ultimately drive landscape response to increasing rates of base-level fall.

ACKNOWLEDGMENTS

This work was funded by the National Science Foundation (NSF) Continental Dynamics program (EAR-0003571), in collaboration with L. Royden and C. Burchfiel at the Massachusetts Institute of Technology, and Z. Chen and T. Fawei at the Chengdu Institute of Geology and Mineral Resources (Sichuan, China). Special thanks are due to J. Frostenson, K. Bradley, J. Johnson, and M. Guoxia for assistance in the field and to A. Cyr and T. Clifton for help with cosmogenic analysis. Thanks also to S. Miller, R. DiBiase, M. Rossi, N. Snyder, L. Sklar, D. Montgomery, G. Stock, and an anonymous reviewer for helpful discussion and feedback.

REFERENCES CITED

Bierman, P., and Nichols, K., 2004, Rock to sediment–Slope to sea with ^{10}Be—Rates of landscape change: Annual Review of Earth and Planetary Sciences, v. 32, p. 215–235, doi: 10.1146/annurev.earth.32.101802.120539.

Bierman, P., and Steig, E., 1996, Estimating rates of denudation using cosmogenic isotope abundances in sediment: Earth Surface Processes and Landforms, v. 21, p. 125–139, doi: 10.1002/(SICI)1096-9837(199602)21:2<125::AID-ESP511>3.0.CO;2-8.

Binnie, S., Phillips, W., Summerfield, M., and Fifield, L.K., 2007, Tectonic uplift, threshold hillslopes and denudation rates in a developing mountain range: Geology, v. 35, p. 743–746, doi: 10.1130/G23641A.1.

Burbank, D., Leland, J., Fielding, E., Anderson, R., Brozovic, N., Reid, M., and Duncan, C., 1996, Bedrock incision, rock uplift and threshold hillslopes in the northwestern Himalayas: Nature, v. 379, p. 505–510, doi: 10.1038/379505a0.

Clark, M., House, M., Royden, L., Whipple, K., Burchfiel, B., Zhang, X., and Tang, W., 2005, Late Cenozoic uplift of southeastern Tibet: Geology, v. 33, p. 525–528, doi: 10.1130/G21265.1.

Clark, M., Royden, L., Whipple, K., Burchfiel, B., Zhang, X., and Tang, W., 2006, Use of a regional, relict landscape to measure vertical deformation of the eastern Tibetan Plateau: Journal of Geophysical Research, v. 111, p. F03002, doi: 10.1029/2005JF000294.

Granger, D., Kirshner, J., and Finkel, R., 1996, Spatially averaged long-term erosion rates measured from in situ–produced cosmogenic nuclides in alluvial sediment: The Journal of Geology, v. 104, p. 249–257.

Heimsath, A., Dietrich, W., Nishiizumi, K., and Finkel, R., 1997, The soil production function and landscape equilibrium: Nature, v. 388, p. 358–361, doi: 10.1038/41056.

Lague, D., Hovius, N., and Davy, P., 2005, Discharge, discharge variability, and the bedrock channel profile: Journal of Geophysical Research, v. 110, F04006, doi: 10.1029/2004JF000259.

Lavé, J., and Avouac, J.P., 2001, Fluvial incision and tectonic uplift across the Himalayas of Central Nepal: Journal of Geophysical Research, v. 106, p. 26,561–26,592, doi: 10.1029/2001JB000359.

Montgomery, D., and Brandon, M., 2002, Topographic controls on erosion rates in tectonically active mountain ranges: Earth and Planetary Science Letters, v. 201, p. 481–489, doi: 10.1016/S0012-821X(02)00725-2.

Niemi, N., Oskin, M., Burbank, D., Heimsath, A., and Gabet, E., 2005, Effects of bedrock landslides on cosmogenically determined erosion rates: Earth and Planetary Science Letters, v. 237, p. 480–498, doi: 10.1016/j.epsl.2005.07.009.

Ouimet, W., 2007, Dissecting the Eastern Margin of the Tibetan Plateau: A Study of Landslides, Erosion and River Incision in a Transient Landscape [Ph.D. thesis]: Cambridge, Massachusetts Institute of Technology, 197 p.

Ouimet, W., Whipple, K., Royden, L., Sun, Z., and Chen, Z., 2007, The influence of large landslides on river incision in a transient landscape: Eastern margin of the Tibetan Plateau (Sichuan, China): Geological Society of America Bulletin, v. 119, no. 11, p. 1462–1476, doi: 10.1130/B26136.1.

Roering, J., Kirchner, J., and Dietrich, W., 2001, Hillslope evolution by nonlinear, slope-dependent transport: Steady state morphology and equilibrium adjustment timescales: Journal of Geophysical Research, v. 106, p. 16,499–16,513, doi: 10.1029/2001JB000323.

Roering, J., Perron, J., and Kirchner, J., 2007, Hillslope morphology and functional relationships between topographic relief and denudation: Earth and Planetary Science Letters, v. 264, p. 245–258, doi: 10.1016/j.epsl.2007.09.035.

Safran, E., Bierman, P., Aalto, R., Dunne, T., Whipple, K., and Caffee, M., 2005, Erosion rates driven by channel network incision in the Bolivian Andes: Earth Surface Processes and Landforms, v. 30, p. 1007–1024, doi: 10.1002/esp.1259.

Snyder, N., Whipple, K., Tucker, G., and Merritts, D., 2003, Importance of a stochastic distribution of floods and erosion thresholds in the bedrock river incision problem: Journal of Geophysical Research, v. 108, no. B2, p. 2117, doi: 10.1029/2001JB001655.

Strahler, A.N., 1950, Equilibrium theory of erosional slopes approached by frequency distribution analysis: American Journal of Science, v. 248, p. 673–696.

von Blanckenburg, F., 2005, The control mechanisms of erosion and weathering at basin scale from cosmogenic nuclides in river sediment: Earth and Planetary Science Letters, v. 237, p. 462–479, doi: 10.1016/j.epsl.2005.06.030.

Whipple, K., and Tucker, G., 1999, Dynamics of the stream-power river incision model: Implications for height limits of mountain ranges, landscape response timescales, and research needs: Journal of Geophysical Research, v. 104, p. 17,661–17,674, doi: 10.1029/1999JB900120.

Whittaker, A.C., Cowie, P.A., Attal, M., Tucker, G.E., and Roberts, G., 2007, Bedrock channel adjustment to tectonic forcing: Implications for predicting river incision rates: Geology, v. 35, p. 103–106, doi: 10.1130/G23106A.1.

Wobus, C., Whipple, K., Kirby, E., Snyder, N., Johnson, J., Spyropolou, K., Crosby, B., and Sheehan, D., 2006, Tectonics from topography: Procedures, promise and pitfalls, *in* Willett, S., Hovius, N., Brandon, M., and Fisher, D., eds., Geological Society of America Special Penrose Publication on Tectonics, Climate, and Landscape Evolution: Boulder, Colorado, Geological Society of America, p. 55–74.

Manuscript received 8 January 2009
Revised manuscript received 8 January 2009
Manuscript accepted 28 January 2009

Printed in USA